The United Nations University

GEOTHERMAL TRAINING PROGRAMME
Orkustofnun, Grensásvegur 9,
IS-108 Reykjavík, Iceland

Reports 2000
Number 2

EXPLOITATION OF THE CONTINENTAL INTERCALAIRE AQUIFER AT THE KEBILI GEOTHERMAL FIELD, TUNISIA

Aissa Agoun
Regional Commissariat for Agricultural Development,
Water Resources Department, C.R.D.A. Kebili,
Kebili 4200,
TUNISIA
aissa@planet-mail.com

ABSTRACT

The "Continental Intercalaire" aquifer is an extensive horizontal sandstone reservoir and ranks as one of the largest aquifers in the world covering 600,000 km^2 in Tunisia, Algeria and Libya. In the Kebili area in southern Tunisia, the geothermal water is about 25-50 thousand years old and of the sulphate-chloride type. The depth of the reservoir ranges from 1,500 to 2,800 m. The piezometric level is about 20 bars and the flow trend is directed from the south and southeast to the north and northwest. During 18 years of exploitation the production rate has reached an average of 4 Mm^3/year and several problems have emerged, the most important being severe corrosion of wellheads, scaling in pipelines and pressure decline in the reservoir. The VARFLOW program was used to simulate production and predict the drawdown until year 2020. The predicted drawdown is about 38 to 60 m, assuming an increase in production by 400 l/s. More detailed water level monitoring and closer cooperation between all producers is recommended. This study concludes that the wellheads are not being corroded from within by the geothermal fluid, but from the outside by a brine that develops due to unfavourable wellhead design and atmospheric conditions.

1. INTRODUCTION

The constraints of climate have driven Mediterranean governments to study and manage available water resources. Population growth and associated economical and social changes have created a new situation at the beginning of the 21st century. Water resources have become so scarce that they limit economic development. The Mediterranean nations must be aware of and learn to avert a potentially disastrous long-term decline in exploitable subterranean water resources. This requires giving priority to the professional management of water resources. Water, or the lack of it, can become a prime factor of war or peace, most notably in the South. In fact the Mediterranean water capacity of 1.250 billions m^3 remains too limited. It represents only 3% of the world resources. Worse, the naturally unequal supplies are divided up between the countries as follows: 72% to the north, 23% to the east and only 5% to the south. And much of the water is not used for consumption. There is also the problem of salinization. Exploitation of the resources must be controlled in order to conserve the geothermal water and reduce disturbances of salinity, temperature and the environment. The policy must be changed to increase

agricultural development with low environmental impact. Tunisian policy is oriented towards agricultural regional development with best possible management of disposable resources. Policies are aimed at assuring the durability of water, the natural, precious main resource of regional development.

The Continental Intercalaire (C.I.) aquifer, which is composed of Upper Carboniferous to Lower Cretaceous rocks, is present beneath an area of about 600,000 km^2 in Tunisia, Algeria and Libya. It constitutes one of the largest groundwater systems in the world. The huge groundwater reservoir is mainly confined to the continental formations of the Lower Cretaceous (Neocomian, Barremian, Aptian, Albian). In Tunisia, the aquifer covers the regions of Kebili, Tozeur, Gabes and the extreme south. The most important production takes place at the Kebili geothermal field where the depth to the top of the reservoir varies from 600 to 2,800 m. Well pressures correspond to 200 metres above wellhead with temperatures of around 70°C. The main utilisation of geothermal water in the Kebili geothermal field is for agricultural purposes; to help irrigate oases, to heat and irrigate greenhouses, in bathing and, in some cases, for animal consumption (Elguedri, 1999). The hot water needs to be extracted by deep wells and cooling through a cooling tower is necessary. Offsetting the growing need for using geothermal water for irrigation, there are several problems encountered during exploitation such as scaling in the pipes, corrosion of anchor casing and some parts of wellheads like valves and monitoring points, and drawdown of the water level due to the increasing water demand.

The present study is concerned with the problem of wellhead corrosion and proposes a new design for wellheads and casing, which can help to avoid external corrosion. Geochemical and isotopic analysis are used to classify the type and determine the origin of the water. An evaluation of reservoir behaviour at the Kebili geothermal field is also carried out and a pressure transient test from a newly drilled well analysed. A prediction of pressure decline in the reservoir in response to increased production is made using the VARFLOW reservoir simulator program.

2. BACKGROUND SETTING

2.1 Geographical setting

The Republic of Tunisia is situated on the long North African shoreline facing the Mediterranean Sea. It covers an area of 164,000 km^2 and has 1,300 km of coastline. Tunisia can be divided into three morphological provinces: i) The Saharan Platform, ii) the mountainous Atlas region and iii) eastern Tunisia. The study area is mostly located on the Saharan Platform, which is a flat plateau dipping gently to the southwest where it is overlain by the sand dunes of the Great Erg. On the northeast side, a series of cuestas limit the lowlands of El Ouara and Jeffara. Very large dry salt lakes, Chott El Djerid, Chott El Fejij and Chott El Gharsa, the latter being 17 m below sea level, form the northern limit. The Saharan Platform, which occupies 60% of Tunisia, is a semi-arid region with an annual rainfall of only 74 mm per year (Japan International Cooperation Agency, 1996).

The Kebili and Tozeur areas have annual mean temperatures above 20°C, mainly because of the very high temperatures in June, July and August. The annual mean evaporation at Kebili is as high as 8.4 mm per day, and high wind velocity is common, especially during the summer months from May to July. The location of the study area is shown in Figure 1.

2.2 Geological setting

The structural framework of Tunisia is characterized by a transition between the Saharan Platform in the south and the alpine folded structures of the Atlas region in the north.

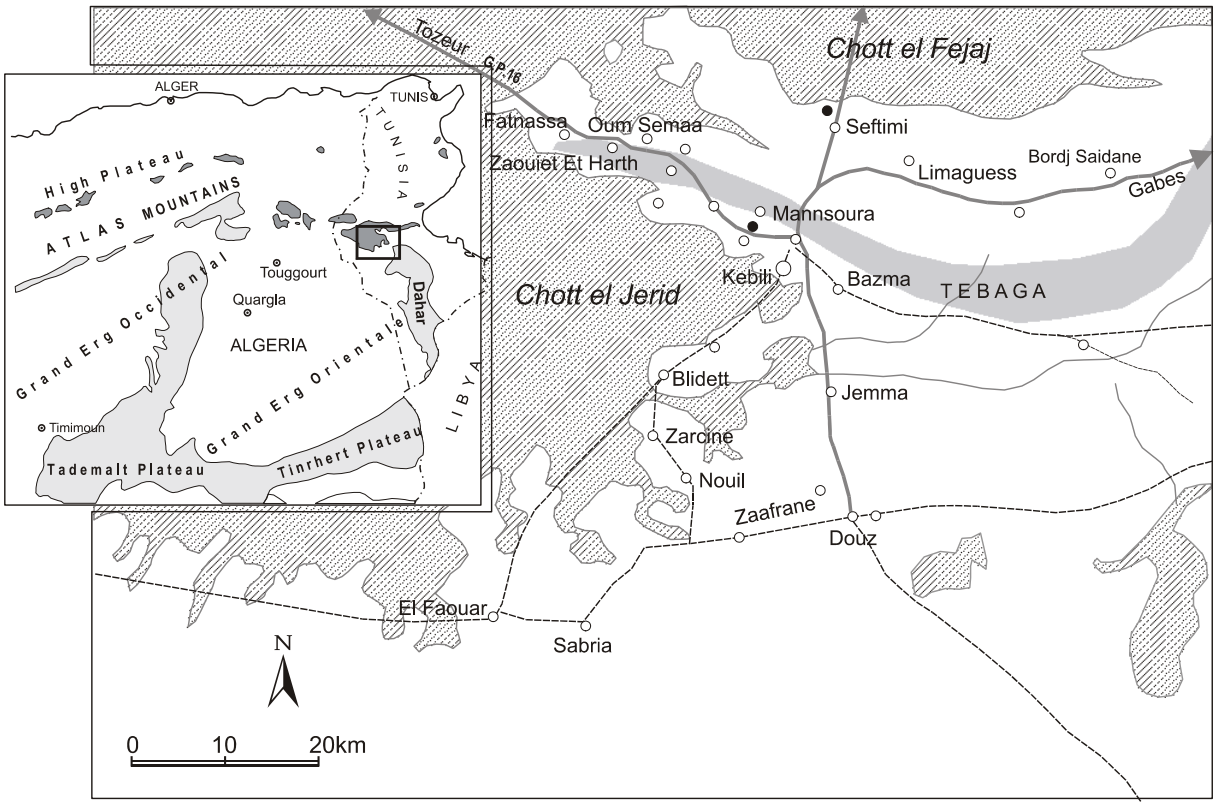

FIGURE 1: Location map of study area

General geology and stratigraphy. As most African countries, Tunisia has a geological basement of Pre-Cambrian age. The basement is not exposed at the surface but has been penetrated by several petroleum wells in the Saharan Platform. The oldest outcropping rocks are of Permian age. There are many outcrops of Triassic rocks but in situ Triassic is known only in the Jeffara plain and at the Libyan border. The Jurassic exhibits great variations in thickness and lithology from north to south. Its maximum thickness exceeds 2,800 m. In the Cretaceous, there is a gradation from neritic, lagoonal and continental lithological facies in the southern Saharan Platform area to open marine and often deep-sea facies in the north. Irregular subsidence, block tilting and salt movements have given rise to complex patterns of thickness and facies since Aptian times. The Cretaceous is divided into two parts by a major basic upper Albian unconformity.

The huge groundwater reservoir of the Continental Intercalaire (C.I.) aquifer is contained within the continental formations of the lower Cretaceous (Neocomian, Barremian, Aptian and Albian). It corresponds to the Asfer formation which is made up of interbedded varicoloured clay or shale, sandstone, and a small quantity of limestone, dolomite and evaporites. Its geology has been described by Castany (1982) among others. The C.I. aquifer consists of several horizons with different permeability and different formation pressures. The main reservoir horizon is the deepest one; it is reached by the main wells.

Kebili is a very large region, but the sands of the Great Erg Oriental desert cover more than half of the area, and the lakes Chott El Djerid and Chott El Fejej occupy considerable areas in the northwest and north. Thus, the area of human activity in this province is limited to a small zone along the eastern shore of Chott El Djerid, which is a slightly hilly country forming a kind of peninsula or island in the Chott.

2.3 Hydrogeology

Ben Dhia and Bouri (1995) divided Tunisia into five geothermal provinces, on the basis of geological and structural characteristics and the distribution of hot springs. In this report we only describe the southern

province that contains the Continental Intercalaire aquifer.

In the southern province, where the Kebili geothermal field is located, the artesian flow rate is usually higher than in the other provinces. The geothermal gradient ranges approximately from 29 to 35°C/km and increases from south to north. There are three main aquifers in this region, the Continental Intercalaire and secondary aquifers within the Jurassic and the Permian. The Continental Intercalaire aquifer covers the regions of Kebili, Tozeur, Gabes and the extreme south and extends to Algeria and Libya. It is characterized by temperatures ranging from 35 to 75°C, pressures of 14-22 bars and salinity of 2.2-4.2 g/l. The geothermal resource potential in the Kebili geothermal field is estimated to be 1,000 l/s (ERESS project, 1972).

The principal areas of current or former recharge are in the South Atlas Mountains of Algeria and Tunisia, the Tinrhet Plateau of Algeria and the Dahar Mountains of Tunisia. The main discharge area is in Tunisia, in the Chotts and the Golf of Gabes. The C.I. aquifer is one of the largest confined aquifers in the world, comparable in scale to the Great Artesian Basin of Australia and covers some 600,000 km^2.

2.4 Main utilization of Continental Intercalaire geothermal water

In the Kebili region and areas further to the south there are 24 wells reaching the different layers of the C.I. aquifer. They are used to supply the oases with water for irrigation after cooling in cooling towers. The geothermal water is also used for heating and irrigating greenhouses. Furthermore, in the Douz region, geothermal water is used for heating two swimming pools and several public bathhouses. In both cases, the return water is used for irrigating the surrounding oases (Ben Mohamed, 1997).

2.5 Previous studies

Several previous studies have addressed the Continental Intercalaire aquifer. UNESCO carried out the study "Etude des Resources des Eaux du Saha Septentrional" between 1968 and 1971 (ERESS project, 1972), with financial aid from UNDP. Ten years later the project was reviewed during RAB project. The studies covered an area of 800,000 km^2 in Tunisia and Algeria. The objectives of these projects were mainly to evaluate the total water demand in these regions by the year 2000 and 2010, to construct a mathematical model of the C.I. aquifer and predict the pressure decline in the reservoir and its economic impact.

According to these studies, the piezometric level of the C.I. is predicted to have fallen by 49-68 m by year 2010 and to 15-40 m below ground in the extreme south of Tunisia. The evaluation and management of water resources of the aquifers in South Tunisia was studied in a separate project in order to obtain an overview of the surface- and groundwater resources in the south, and forecasts of the groundwater conditions in the future. The volume of groundwater resources in the south is about 46% of all groundwater resources in Tunisia. The project "Recharge characteristics and groundwater quality of the grand Erg Oriental Basin" was started in 1994 as a cooperative project between the United Kingdom (British Geologic Survey), Algeria (C.D.T.N), and Tunisia (D.G.R.E. and E.N.I.S.). The main goal of this project is to define the limits of sustainable groundwater development in the aquifer system of the Grand Erg Oriental underlying eastern Algeria and southern Tunisia. This project is for all the aquifers in this area and aims at determining the modern rates of recharge and the interface between recent recharge and palaeowaters. Finally, the study "Sahara and Sahel Observatory" commenced in 1999. The main objectives were to evaluate and expand previous studies of the deep aquifers (C.I., C.T. and Djeffara) in East Algeria, South Tunisia and, for the first time, Libya.

3. DATA

3.1 Wells

Table 1 lists the 25 wells drilled in order to exploit the C.I. aquifer. The average exploited thickness of the reservoir is about 100 m. Four of the wells do not penetrate the main feed zone. The geographical location of the wells is shown in Figure 2. UTM locations are based on a transformation of the coordinate data from degrees to km units as given in Appendix 1. The reservoir is tapped by wells reaching depths of up to 2,800 m. 37 wells have been drilled in the field between 1952 and 2000. During 1999-2000 four wells were drilled in the area, the deepest one, well 22, reached 2,400 m depth.

TABLE 1: Characteristics of wells producing from the C.I. aquifer

Well	Drilled	Latitude (N)			Longitude (E)			Elev.	Depth	Slotted screen		S.W.L.**	Yield
no.	year	deg.	min.	sec.	deg.	min.	sec.	(m a.s.l.)	(m)	Depth (m)	H(m)	(m-wh)	(l/s)
1	1983	33	46	39.6	8	50	6.6	27	1420			20.9	38
2*	1984	33	47	28.8	8	46	4.6	24	1405	900-1098	198	38.6	28
3*	1985	33	43	25.4	8	56	47.4	28	2200	1700-1900	200	56.5	14
4	1985	33	47	9.1	8	49	49.9	55	2200			205.9	79
5	1985	33	47	19.4	8	47	49.6	35	2229			212.2	84
6	1986	33	46	53.9	8	51	35.8	50	2310	2178-2304	126	202.3	86
7	1986	33	47	51.1	9	0	51.8	53	1987	1668-1788	120	178.5	52
8	1985	33	46	6.4	9	4	46.3	80	1752	1568-1730	162	152.9	46
9	1986	33	47	12.4	9	15	23.6	48	1621	1268-1400	132	137.3	68
10	1986	33	41	46.5	8	59	5.3	50	2580	2286-2558	172	176.0	77
11	1986	33	33	11.3	9	0	46.7	45	2192	1928-2078	150	217.0	126
12	1986	33	26	9.7	9	1	58.8	65	2080	1926-1994	68	198.2	36
13	1992	33	43	6.8	8	56	36.7	23	2682			197.3	30
14	1992	33	47	50.8	8	41	33.2	24	2480			217.5	71
16	1994	33	40	54	9	0	30.2	50	2800	2578-2774	196	139.3	70
17	1994	33	48	41.1	8	43	21.8	23	2500	2100-2250	150	205.0	70
18	1994	33	24	27.6	9	0	52.1	60	2020			186.0	70
19	1993	33	20	14.5	8	40	1.8	50	1894			211.7	30
20	1999	33	47	50	8	49	60		1104			12.1	54
21	2000	33	45	50	8	51	10		1099			5.3	83
22	2000	33	47	1	8	51	55	60	2400	2179-2292 2298-2309	124	180.0	219
23	1999	33	44	00	8	51	50		1245			21.2	54
Sa	1985	33	45	9.7	9	17	41.9	80	800	744-751	7	73.6	28
KG3	1980	32	59	12.5	9	38	21.2	198	680	628-679	51	69.4	70
KG2	1963	32	59	13	9	38	21.1	198	676				57
St2*	1961	33	48	0.7	9	0	43.2	52					7
St3*	1961	33	48	0.7	9	0	43.2	52	1005			56.6	13
Mbs	1986	36	48	0	8	11	0	236,1	680	620-627	7	57.5	6

* Well does not penetrate the main feed zone; ** Static water level.

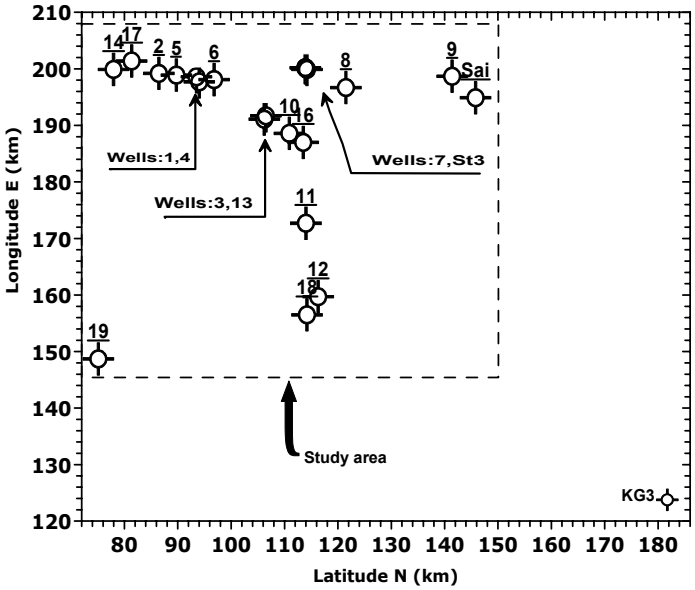

FIGURE 2: Geographical distribution of production wells in the study area

Monitoring of the piezometric head of the aquifer through wellhead pressure measurements at different flow rates has been very limited, because such measurements require that production be stopped for more than 24 hours, and with the problem of scaling and corrosion, the valves cannot be closed completely. The available data on wellhead temperatures and salinity are shown in Table 2. The history of production and associated pressure decline (drawdown) is shown for each well in a table in Appendix 2.

TABLE 2: Physical parameters of the geothermal fluid at the wellhead

Well	T		TDS		Well	T		TDS	
no.	(°C)	(Year)	(mg/l)	(Year)	no.	(°C)	(Year)	(mg/l)	(Year)
1	46.0	1994	2800	1994	18	44.7	1994		1994
2	45.5	1994	2300	1994	19	51.0	1999		1999
3	52.2	1994	3000	1994	20		1999		1999
4	70.0	1996	2270	1996	21		1999		1999
5	70.9	1996	1840	1996	22	70.0	2000	3200	2000
6	71.0	1996	2590	1996	23		1999		1999
7	72.5	1996	2440	1996	Sad	55.0	1998	2900	1994
8	72.5	1996	2450	1996	KG3b	34.3	1991	4500	1994
9	68.0	1996	2670	1996	KG3	34.0	1994	4500	1994
10	70.9	1996	2410	1996	St2			3100	1994
11	59.0	1996	2870	1996	St3	44.3	1994		
12	53.0	1996	2320	1996	OF2	33.7	1994	3300	1994
13	62.0	1999	2300	1994	OF3	39.6	1994		
14	71.0	1999	2160	1996	Mch	45.0	1994	5500	1994
16	64.0	1994		1994	Mhb	33.0	1999		
17	68.0	1994		1994					

3.2 Chemistry

The present geochemical study is based on 12 samples obtained from selected geothermal wells in the study area in May 1994. The major chemical composition of the samples is shown in Table 3. The analytical results for trace element analysis are shown in Appendix 3. Samples for isotopic analysis were taken at the outlet of the wells in the cooling tower, i.e. before the water is released to the irrigation networks. On-site analysis included total alkalinity (HCO_3), pH and dissolved oxygen (DO). Samples intended for laboratory analysis were collected and analysed by the British Geological Survey (BGS) in the UK. Laboratory and international reference materials were used to check the accuracy of each analysis. Samples for stable isotope analysis (δD, $\delta^{18}O$) were analysed by gas source mass spectrometry. These analyses were also carried out by BGS.

TABLE 3: Analytical results for major elements (mg/l) and isotopes (‰ SMOW) in water samples from the C.I. aquifer (Edmunds et al., 1995)

Well no.	pH	Ca	Mg	Na	K	SO_4	Cl	HCO_3	NO_3	TDS*	CO_2	DO**	Ionic. ball. (% diff.)	δD (‰)	$\delta^{18}O$ (‰)
4	7.9	208.4	97	375	12	677	667	122	6.2	2,270	88	4.3	2.77	-60	-8,8
5	8.0	188.4	105	388	55	562	567	293	16.7	1,840	211	4.3	3.47	-81	-8,2
6	8.1	258.5	80	382	48	630	702	232	3.7	2,590	167	4.8		-60	-8,4
7	8.1	210.4	103	354	45	690	677	183	1.8	2,440	132			-59	-8,4
8	8.3	240.0	103	287	36	931	497	86		2,450	62		2.54	-61	-8.5
9	8.3	220.4	130	414	50	816	753	238	2.5	2,670	172		0.97	-59	-8,1
10	8.2	248.5	85	402	41	745	617	201	3.7	2,410	145	3.7	-1.17	-64	-8.4
11	8.2	250.5	73	598	42	792	876	256	3.7	2,870	185		2.92	-54	-8,6
12	8.2	232.4	66	418	44	696	674	110	8.7	2,320	79		-7.87	-80	-8,7
14	8.0	228.0	145	265	28	816	568	123		2,160	89	4.5		-58	-8,1
Mbs	8.0	336.0	137	612	43	974	1140	154		4,600			1.75	-57	-7,7
KG3	7.7	434.0	222	8.7	32	1400	1460	184		4,500			4.26	-47	-6,8

* Total dissolved solids; ** Dissolved oxygen

3.3 Corrosion phenomena

A typical wellhead design for wells, reaching the C.I. aquifer is shown in Figure 3. The wellhead is anchored in a 13 ⅜" production casing. Corrosion has begun to affect several of the C.I. wellheads (wells 4, 5 and 9). Figure 4 shows an example of corrosion of the top of the anchor casing of well Sa.

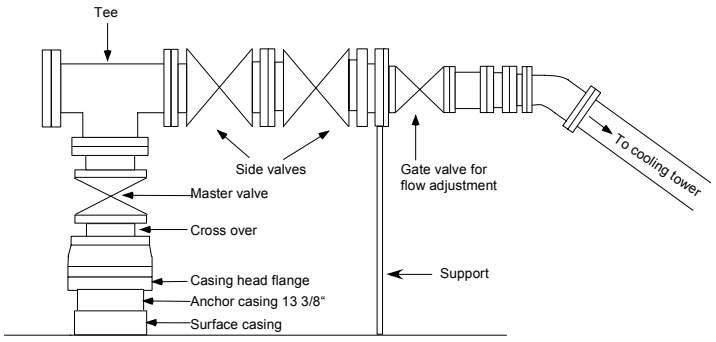

FIGURE 3: Typical wellhead design in the Kebili area

Prevalent ideas on the origin of corrosion deem geothermal water a corrosive agent. It is, however, important to consider a possible external source. In fact, several important factors leading to corrosion such as moisture, high temperature and presence of oxygen and salts characterize the external environment.

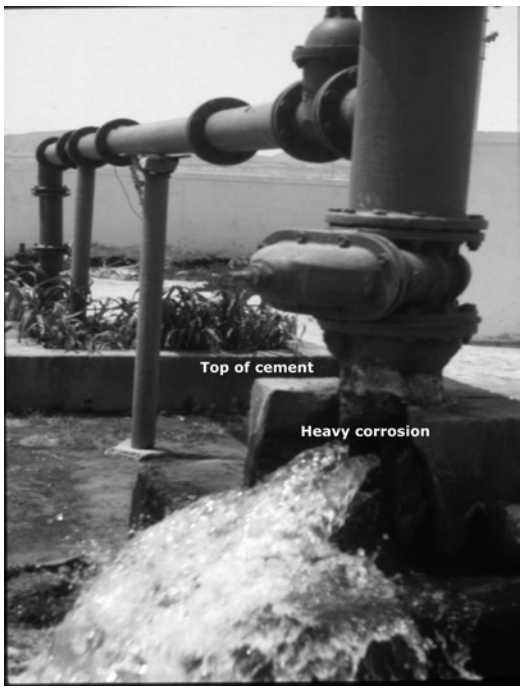

FIGURE 4: Wellhead of Sai with corrosion

4. WATER CHEMISTRY

4.1 Type of water

For the classification of thermal waters and the identification of processes that have affected their composition, the triangular diagram Cl-SO_4-HCO_3 is commonly used. The plot is obtained by calculating the sum S of the concentration C (mg/l) of all three constituents (Giggenbach, 1991), $S = C_{Cl} + C_{HCO3} + C_{SO4}$ and then calculating the %-Cl, %-HCO_3 and %-SO_4. Figure 5 shows that the data points for water from wells reaching the C.I. aquifer plot in the middle of the Cl and

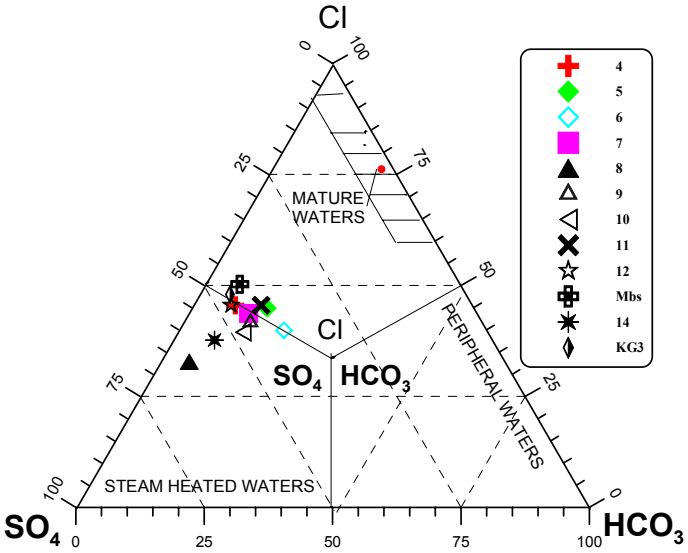

FIGURE 5: The Cl-SO_4-HCO_3 triangular diagram for water chemistry

SO_4 areas, but some of this water shows relatively high concentrations of SO_4. The reservoir rocks are mainly composed of sandstone with gypsum and anhydrite intercalations and gypsum and anhydrite minerals are the likely source of SO_4. The Cl content ranges from 500 to 1,200 mg/l and probably derives from marine formation water. However, the concentration of I is lower than expected from a marine influence. The temperature and the chemical composition have not changed significantly with time. Evaporite dissolution and redox equilibrium processes are thought to control the water quality and the distribution of salts. The quality of irrigation water is governed mainly by four characteristics: total concentration of soluble salts, ratio of sodium to other cations, concentration of boron and other toxic elements and the concentration of bicarbonate. The C.I. water quality is close to the limits of potability and, therefore, well within the limits of use for agriculture. In fact, it is well suited for agricultural uses.

The amount of dissolved oxygen was obtained from on-site analyses and is not so accurate. In fact, the high concentration of oxygen can be of atmospheric origin due to the location where the samples were taken. The solubility of oxygen in distilled water in contact with air depends on temperature. Oxygen saturated water has a concentration of about 3.8 mg O_2/kg (Appendix 4), which is the same concentration as measured in the samples. The water from the C.I. aquifer is far from being saturated by atmospheric oxygen. It is recommended to take a representative sample of water from each well through a sampling point in the surface pipeline a distance of 1.5 m from the wellhead to avoid the turbulent water flow.

4.2 Origin of the water

Radiocarbon analysis has shown that radiocarbon is present at between 2 and 10 pmc which leads to the conclusion that the water was recharged during the late-Pleistocene, in the period 25,000 year BP, corresponding to the last glacial maximum in Europe (Edmunds et al., 1997).

The stable isotopes of hydrogen and oxygen are used to obtain more information about the origin and the possibility of recharge of this aquifer. Figure 6 shows the relationship between δD and $\delta^{18}O$ of the geothermal water from the C.I. aquifer in the Kebili area. The data points are concentrated along the meteoric line of Craig (1961), indicating a meteoric origin of the geothermal water. $\delta^{18}O$ ranges from –7.5 to -9% and this signature is characteristic of palaeowaters in northwest Africa.

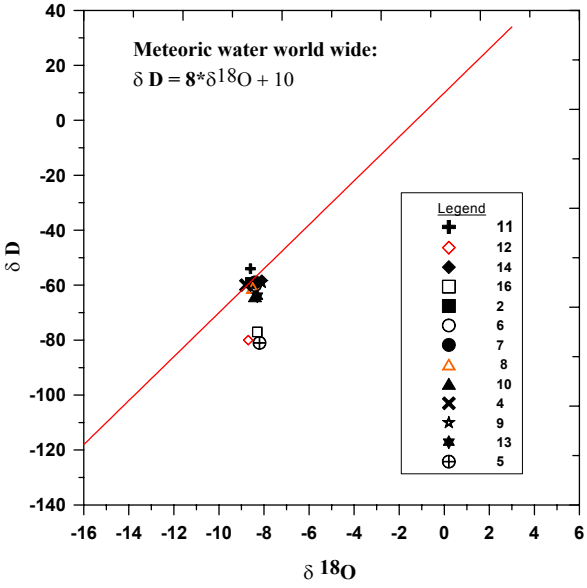

FIGURE 6: A δD vs. $\delta^{18}O$ plot for the collected samples

An estimate of the current recharge of the C.I. aquifer water using these isotopes shows that the groundwater reserves are non-renewable (Edmunds et al., 1997).

5. CORROSION

5.1 Basic theoretical background

Corrosion is basically a chemical or electrochemical destructive process (Hayashi, 1988), in which four conditions must be present: 1) There must be a positive or anodic area, referred to as the "anode"; 2) There must be a negative or cathodic area, referred to as the "cathode"; 3) There must be a path for ionic current flow, or "electrolyte"; 4) There must be a path for electronic current flow, which is normally a "metallic path".

The electrical potential between the anode and cathode causes the corrosion current to flow. The anode is the area that suffers metal loss and corrosion. The amount of metal that will be removed is directly proportional to the amount of current flow.

The rate of uniform attack is reported in various units, the usual terminology in the USA being inches penetration per year (ipy) and milligrams per square decimetre per day (mdd). In humid environments several factors affect the process of corrosion. The following are among the principal ones:

Effect of dissolved oxygen. At ordinary temperatures in natural or near-natural water, dissolved O_2 is necessary for considerable corrosion of iron. In air-saturated water, the initial corrosion rate may reach a value of about 100 mdd. The rate diminishes when an iron oxide (rust) film is formed and acts as a barrier to O_2 diffusion. Since the diffusion rate at steady-state is proportional to the oxygen concentration, the corrosion rate of iron is also proportional to oxygen concentration. At critical concentration the corrosion rate drops again to a low value (Uhlig, 1967). In distilled water, the critical concentration of O_2 above which corrosion decreases again is about 12 ml O_2/liter. This value increases with dissolved salts and with temperature, and decreases with increase in fluid velocity and pH (at pH = 10, the critical concentration is 6 ml O_2/liter of air-saturated water).

Effect of temperature: When corrosion is controlled by diffusion of O_2, the corrosion rate at a given O_2 concentration approximately doubles for every 30°C rise in temperature (Uhlig, 1967). In an open system, allowing O_2 to escape, the rate increases with temperature to about 80°C, and then falls to a very low value at the boiling point. This decrease is related to the decreasing O_2 solubility in water as the temperature is raised. In a closed system, the corrosion rate continues to increase with temperature until all oxygen is consumed.

Effect of pH: The corrosion of iron at room temperature by aerated water is related to the range of pH. At pH between 4 and 10, corrosion is independent of pH, and depends only on how rapidly oxygen diffuses to the metal surface. Within the acid region (pH<4) the ferrous oxide film is dissolved, and iron is more or less in direct contact with the aqueous environment. The increase of the reaction rate is the sum of both an appreciable rate of hydrogen evolution and oxygen depolarisation. Above pH 10, increase in alkalinity of the environment raises the pH of the iron surface. The corresponding corrosion rate decreases because iron becomes increasingly passive in the presence of alkalis and dissolved oxygen. Oxygen concentration, temperature and water velocity alone determine the reaction rate (Uhlig, 1967).

Effect of dissolved salts: Higher NaCl concentrations increase iron corrosion in air-saturated water at room temperature. The corrosion rate reaches a maximum at 3% NaCl (sea water concentration) and then decreases, because O_2 solubility in water decreases continuously with NaCl concentration. The protection mechanism afforded by hard water is the natural deposition of a thin diffusion barrier film composed largely of calcium carbonate, $CaCO_3$. The film retards diffusion of O_2 to the metal surface.

Metallurgical factor: Whether steel is manufactured by the Bessemer or open-hearth process, is wrought iron, or cast iron, makes little or no difference to the corrosion rate in natural water. The same statement applies to corrosion in a variety of soils because factors determining the corrosion rate underground are similar to those of total submersion. In general, therefore, the least expensive steel or iron of given cross-sectional thickness which has the required mechanical properties is the one that should be specified.

In summary, it can be said that at normal temperatures iron will not corrode appreciably in the absence of moisture. The presence of oxygen is also essential for corrosion to take place in ordinary water. Oxygen alone will cause considerable corrosion in acid, neutral, or slightly alkaline water; in natural waters, the rate of corrosion is almost directly proportional to the oxygen concentration, if other factors do not change. Corrosion in acid solutions is much more rapid than in neutral solutions. In acid solutions and concentrated solutions of alkalies, hydrogen gas is usually evolved from the surface of the metal during corrosion. The products of corrosion consist, mainly, of black or green ferrous hydroxide next to metal; and reddish-brown ferric hydroxide (rust) forming the outer layer (Uhlig, 1967).

Typical chemical reactions of the corrosion process: The most common type of corrosion is electrochemical where the metal ions go into solution at anodic areas in amount equivalent to the reaction at the cathodic area. For the corrosion of iron and steel the anodic reaction is

$$Fe \Rightarrow Fe^{++} + 2e^{-} \tag{1}$$

The rate of the reaction is controlled by the cathodic reaction, which depends on the pH of the water

$$O_2 + 2H_2O + 4e^{-} \Rightarrow 4OH^{-} \tag{2}$$

and

$$2H^{+} + 2e^{-} \Rightarrow H_2 \tag{3}$$

Reactions 2 and 3 permit Reaction 1 to proceed with the accumulation in the solution of Fe^{++}, which is oxidized and precipitated as rust by

$$2Fe^{++} + 0.5O_2 + H_2O \Rightarrow 2Fe^{+++} + 2OH^{-} \Rightarrow \textit{Insoluble ferric hydroxide (rust)} \tag{4}$$

In general, the primary factors which determine the tendency of a metal to corrode and, thus, influence its initial rate of solution (Reaction 1), have to do with the metal (or alloy) itself; the secondary factors which influence the rate of subsequent reactions, more with specific environments. If the surface of the metal is immersed in a solution that is in any way non-homogeneous, there will be local differences of effective electric potential of the metal. In a solution, this means that the chemical and physical homogeneity and texture of the metal surface affects the rate of corrosion (Speller, 1935). The hydrogen ion concentration (pH) exerts another effect, somewhat indirectly, in that it changes the solubility of ferrous hydroxide, and other substances which may be precipitated, and the resulting protective film.

5.2 Description and analysis of wellhead corrosion in C.I. wells

For the wells reaching the Continental Intercalcaire aquifer, corrosion occurs on the outside of the anchor casing, mainly at contact with the ground surface. The corrosion results in a reduced casing thickness. Figure 4 shows the location of the most extensive corrosion in the anchor casing. After 15 years of operation, corrosion also appears at the top of the anchor casing. An important source of corrosion is thought to be differential aeration of the electrolytes (commonly soil). In a situation where part of a structure is in well aerated soil, and an adjacent part is in oxygen-starved (poorly aerated) soil, the part of the structure in the well-aerated soil will be the cathode and the part of the structure in the poorly aerated soil will be the anode.

In external corrosion the main element that should be taken into consideration is the role of oxygen and not only the geothermal fluid in the well. To replace the anchor casing is very costly. The soil is enriched in gypsum and salts, which participate in corrosion of the anchor casing from the outside where it makes contact with humid soil. On a hot day the temperature of the surface contact area is 40°C but during the night decreases to 2-10°C. This temperature contrast also contributes to the outside corrosion. The moisture in the air, which contains oxygen, is in places directly in contact with the anchor casing. As shown in the previous chapter, oxygen and moisture are the main factors accelerating the corrosion rate. The wellhead and the exposed part of the anchor casing are exposed to meteoritic conditions without any protection. It is important to consider these factors as well as the thickness of the anchor casing.

5.3 Protection against corrosion

As described, the main causes of corrosion are probably external factors such as moisture around the wellhead, salts and the temperature at the contact with the anchor casing. The wellhead and anchor casing design should therefore meet certain requirements. In fact, where conditions are likely to cause corrosion of the surface casing, the following preventive measures should be taken.

Corrosion mitigation	Specific remedy
1. Removal or chemical modification of the corrosive environment, or the addition of an inhibiting film for protecting the anchor casing surface.	Keep the wellhead and annulus **dry** by filling annulus with cement. Install breather tube. Repair any leakage**.**
2. The provision of sacrificial thickness to achieve the required casing life.	Topmost pipe of anchor casing (13⅜") should have extra wall thickness minimum 15-20 mm.
3. Application of a resistant covering over the casing surface, e.g. thick cement sheath, chromium plating or a suitable, high-temperature resin coating (New Zealand standard, 1991).	Cover wellhead and anchor casing with high build painting or shrinking plastic film.

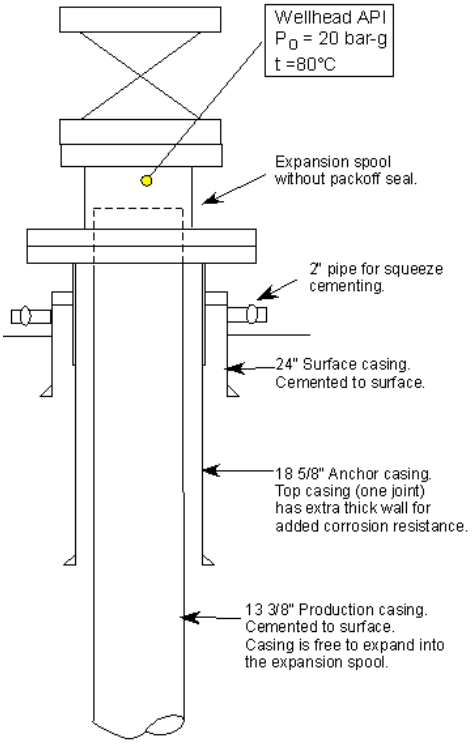

FIGURE 7: Special thick-walled anchor casing for added corrosion protection

The casing design should take into account the effects of all combinations of pressure, temperature and temperature changes. The topmost pipe in the 13⅜" (339.7 mm) anchor casing string should have an inside diameter of 315.35 mm and a nominal weight of 88.20 lb/ft. The minimum wall thickness should be 20 mm and the steel grade should be J55 or K55 (Gabolde and Nguyen, 1999). Figure 7 shows a typical special thick-walled anchor casing to minimize the corrosion effects.

6. AQUIFER

6.1 Well design

Because of the uncompacted nature of the aquifer sand, the producing zone is filtered with a 6 ⅝" slotted metal screen made of stainless steel. This diameter is chosen in order to limit the effect of turbulent flow. A liner hanger packer is used to prevent sand entering between casings. The casing steel grades API J55, K55 and N80 are used for production and intermediate casings. A typical well casing design is shown in Figure 8.

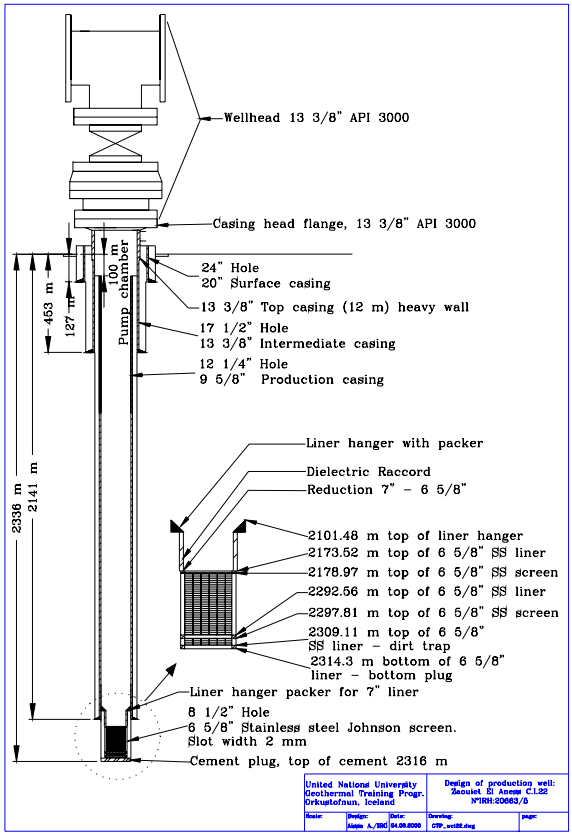

FIGURE 8: Casing strings and slot screen for a typical well (well 22)

6.2 Well test

In May 2000, a new well was drilled and tested for ca. 24 hours. The data collected are presented in Table 4. The initial pressure was 18.85 bars. Production and pressure decline data from this test were used to estimate the hydro-geological properties of the C.I. aquifer. Because of a variable flow rate, Jacob's method was used to model the relationships between drawdown and variable flow rate. The relation can be written (Todd, 1959) as

$$\Delta H = h_o - h_w = \frac{Q}{2\pi kh} \ln\frac{r_o}{r_w} + CQ^n \qquad (5)$$

where r_o = Radial distance from the well [m];
r_w = Well radius [m];
k = Permeability [1 D = 10^{-12} m^2];
h = Thickness of aquifer [m];
Q = Flow rate [m^3/s];
ΔH = Drawdown [m].

A value of $n = 2$ that is reasonable (Todd, 1959). From Equation 5 it follows with in the case of turbulent flow

$$\Delta H/Q = B + CQ^2 \qquad (6)$$

C is a constant governed by the radius, construction, and condition of the well whereas B is mostly governed by the transmissivity, kh/μ, of the reservoir and its thickness. B can be written as

$$B = \frac{\ln(r_o/r_w)\mu}{2\pi kh\rho g} \quad (7)$$

where g = Acceleration due to gravity 9.8 [m/s^2];
μ = Dynamic viscosity of geothermal water: 0.000405 [kg/ms];
ρ = Density of water = 980 [kg/m^3].

TABLE 4: Data from testing of well 22 (C.R.D.A., 1999)

Time (H)	Q (m^3/s)	W.L. (m)	ΔH (m)	ΔH/Q (m-^{2}/s)	Temp. (°C)
0	0	188.5	0	0	
4	0.057	180.0	8.5	0.149	68
4	0.075	165.0	23.5	0.310	68
4	0.107	140.0	48.5	0.451	68
4	0.139	110.0	78.5	0.564	68
4	0.172	51.0	137.5	0.797	68
4	0.219	3.5	185.0	0.845	70

A plot of ΔH/Q vs. Q is shown in Figure 9 together with the best fitting straight line. From the intercept of this line with the $\Delta H/Q$ axis, B = 30 s/m^2, from which the permeability thickness kh, can be calculated. Indeed, with r_w = 0.11 m and r_o = 1000 m the permeability thickness, is about 2×10^{-9} [m^3]. Consequently, the permeability, k, is 2×10^{-11} [m] assuming an average thickness of 100 m. The transmissivity $T = kh/\mu$ is about 4.9×10^{-6} [m^3/Pa/s].

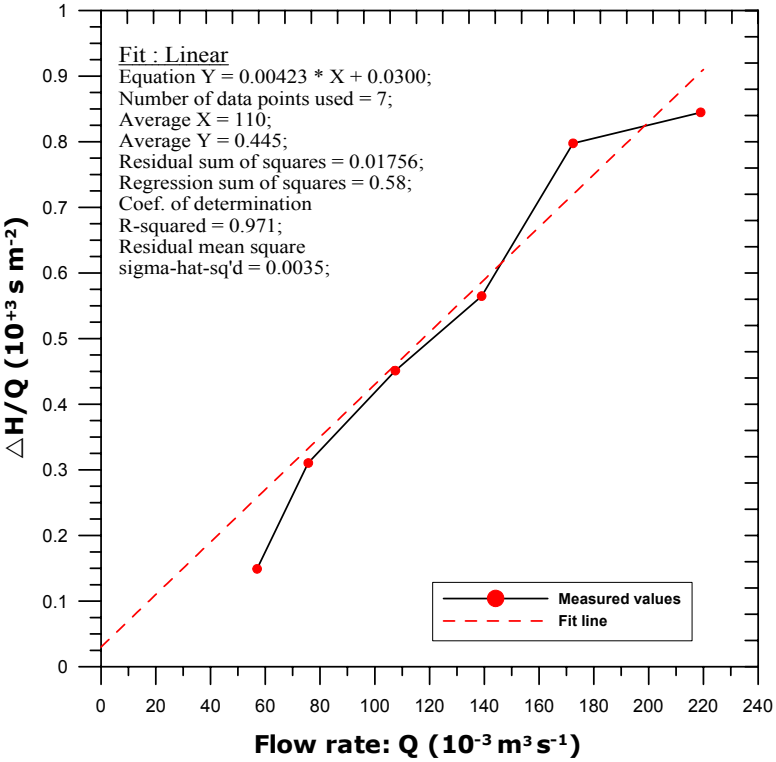

FIGURE 9: Analysis of a pressure transient by a $\Delta H/Q$ vs. Q plot

A simulation of storativity was carried out in order to compare it with the results given by the program VARFLOW. The reservoir rock of the C.I. aquifer is made of sand interbedded with clay, gypsum, anhydrite and lignite with an estimated porosity of 4%. Assuming a confined reservoir, the total formation compressibility "c_t "can be calculated from the following equation

$$c_t = \phi c_w + (1-\phi)c_r \quad (8)$$

where ϕ = Porosity [%];
c_w = Fluid compressibility [Pa^{-1}];
c_r = Rock compressibility [Pa^{-1}];
ρ_w = Fluid density [kg/m^3].

The storativity can then be estimated from (Matthews and Russell, 1967)

$$s = c_t h = h(\phi c_w + (1-\phi)c_r) \quad (9)$$

With a porosity ϕ = 4%; $c_w = 5\times10^{-10}$ Pa^{-1}, ρ_w = 980 kg/m^3, h = 100 m and $c_r = 2.5\times10^{-11}$ Pa^{-1}, the storativity is estimated to be $s = 18.5\times10^{-9}$ kg/Pa^{-1}m^3. The C factor is about 4230 [m/(m^3/s)^2], which is not as important in view of the diameter of the casing and the depth of the reservoir.

6.3 History of production and pressure decline

The production and pressure decline history of the C.I. aquifer in the Kebili area is shown in Figure 10. The data show a general decrease in pressure with increasing production. Figure 10 shows three periods of production. The first was during 1982-1984, when about 80 l/s were extracted. Few pressure measurements are reported from this period but the drawdown was small. The second period was during 1984-1991, when extraction seldom rose above 900 l/s and drilling activity was at a maximum. In this period, the drawdown was monitored and data show a pressure drop of about 0.5 bars/year in several wells. The last period, 1991-1999, shows a large pressure drop of about 2 bars/year in most wells in response to an average mass extraction of 1,200 l/s from 29 wells operating in the region (C.R.D.A., 1999). Production was limited through the use of a water saving system under which farmers were encouraged to install PVC pipelines for irrigation and to prevent water wastage due to infiltration and evaporation.

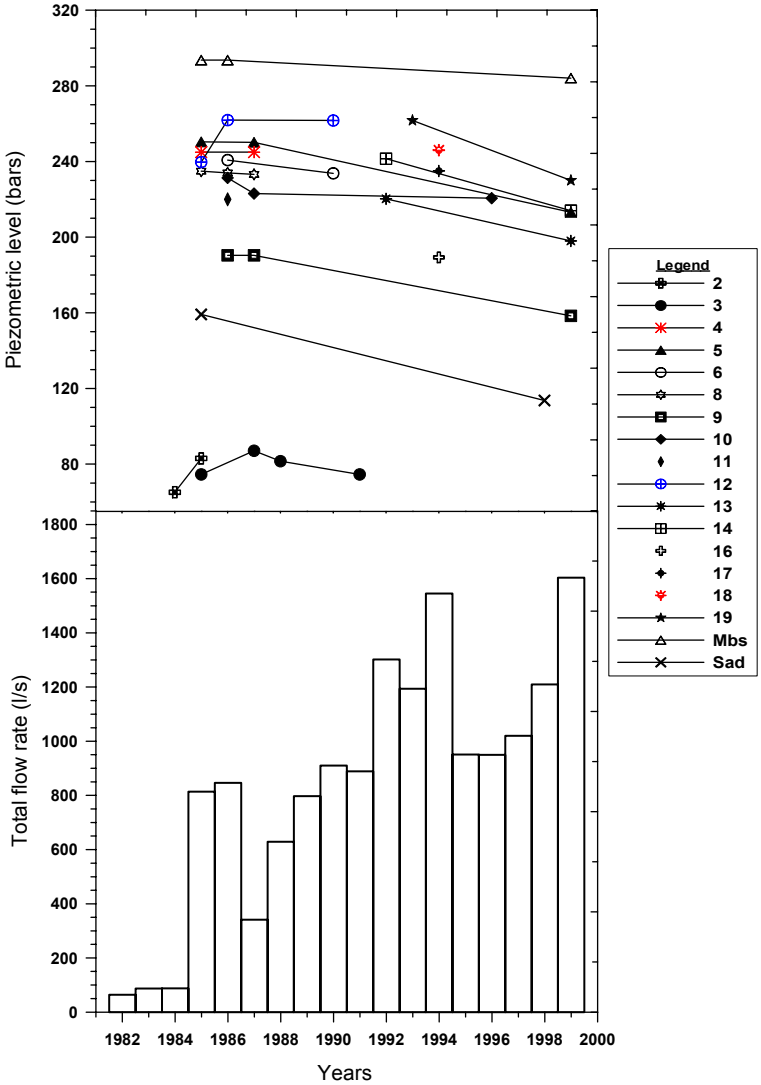

FIGURE 10: Temporal variation of production and piezometric level

6.4 Conceptual model

A conceptual reservoir model is used as a simplified description of the main elements of a geothermal system as far as they are known from exploration. The conceptual model serves as a basis for the construction of numerical reservoir models to define the geometry of the reservoir and locate boundaries, recharge sites and discharge zones. Available data such as temperature, salinity, the depth to the top of

the producing zone and the piezometric level for two periods were used to construct a conceptual model of the C.I. aquifer in the Kebili geothermal field. According to the isotopic data, the meteoric water percolates deep into the crust and gains heat from the geothermal gradient. The aquifer is tabular with a slope ranging from 5 to 10° to the south. The pressure and temperature increase with the depth of the reservoir and according to the geothermal gradient (25-30°C/km).

Figure 11 shows a contour map of wellhead temperatures. Since no data are available for the southern region, the plot was limited to the northern zone containing more wells. This plot shows that the temperature increases from southeast to northwest. Figure 12 shows that the depth to the top of the reservoir increases from the east to the west, the deepest part (2,500 m) being located in the northwest. Low wellhead temperatures found in the southeast (below 30°C) are not shown in this plot, but high temperatures of about 70°C are found in the northwest part of the study area.

The salinity, or the total dissolved salts, plotted in Figure 13 shows a decrease from the southeast to the northwest; i.e. it varies inversely with depth and temperature. This increase is considered to be the result of the dissolution of halite and gypsum in the reservoir formation. This solubility is inversely proportional to aquifer pressure.

Production data for 18 years are summarized in Appendix 2. Figures 14 and 15 show the wellhead pressure distribution in 1986 and 1999, respectively. Both of them indicate that the main flow of geothermal fluid is from the southwest to the northeast. The contours open to the south. A comparison of the two plots of 1986 and 1999 shows a decrease in the piezometric level in response to increased total flow production. After 13 years, the 215-m a.s.l. contour line has moved to the southwest by 20 km, i.e. by 1.5 km/year.

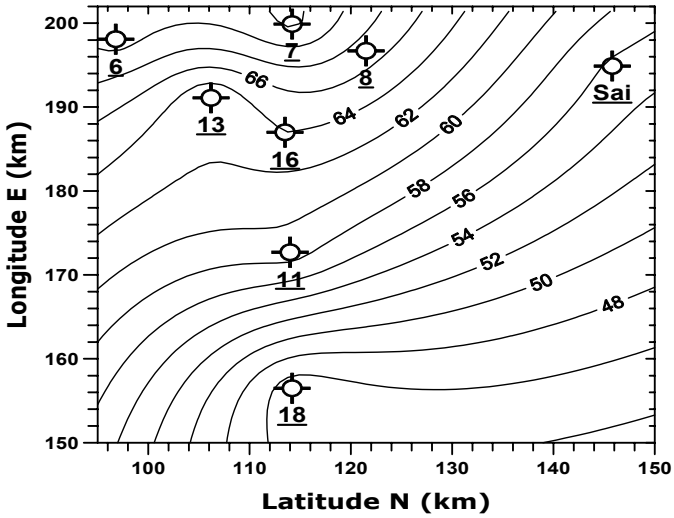

FIGURE 11: Wellhead temperature plot (°C)

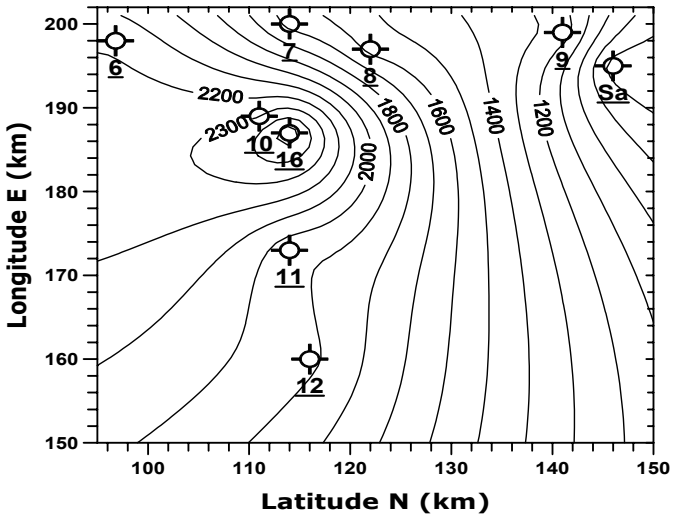

FIGURE 12: Depth to the top of the producing zone (m)

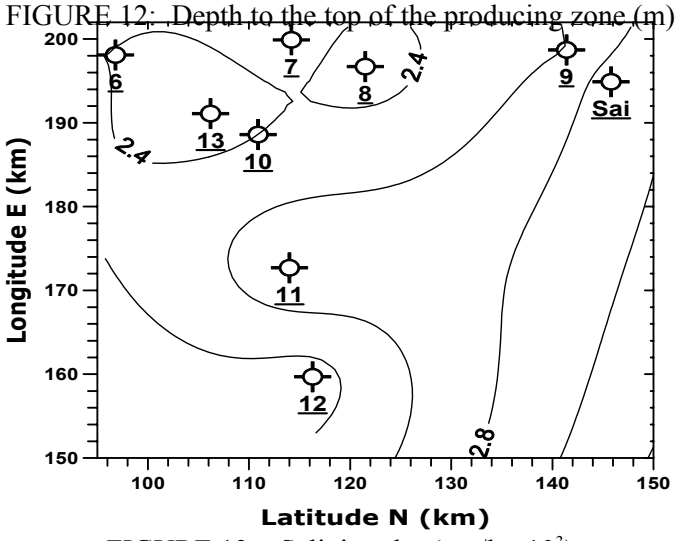

FIGURE 13: Salinity plot (mg/l × 10^3)

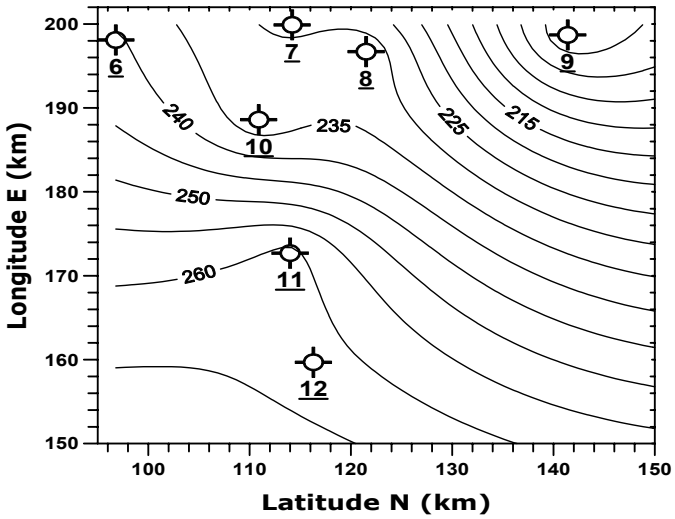

FIGURE 14: Piezometric level in 1986 (m a.s.l.)

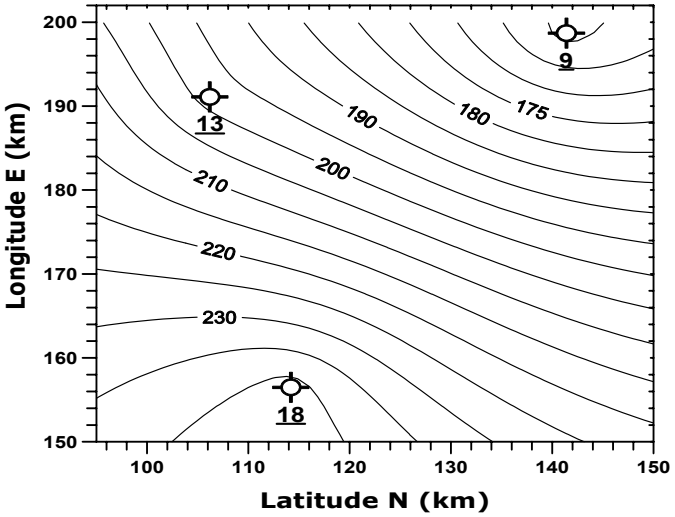

FIGURE 15: Piezometric level in 1999 (m a.s.l.)

6.5. Numerical model

An important aspect of the assessment of an aquifer is the development of a numerical model. The main purpose of such a model is to help to predict the performance of the reservoir under different exploitation conditions and production potential. Distributed parameter modelling techniques are complex tools which simulate many measurable parameters (pressure, flow rate, etc.). The modelling requires an accurate conceptual model based on extensive field data (Axelsson and Björnsson, 1993).

The computer program VARFLOW in the icebox software package was used for calibration of the reservoir parameters through modelling and simulation of the production history of the reservoir. VARFLOW calculates pressure changes in response to fluid production from an idealized reservoir system. This software allows the use of multiple wells with variable flow rates. The governing equation describes the pressure changes (ΔP) caused by production from a single well with a variable flow rate, q. It is written in integral form as follows:

$$\Delta P(t) = \frac{\mu}{4\pi kh}\int_{t_n}^{t_{n+1}} \frac{q(\tau)}{t-\tau}\exp\left[\frac{-\mu c_t r^2}{4k(t-\tau)}\right]d\tau \qquad (10)$$

where ΔP = Pressure change at time t due to the flow rate $q(\tau)$ for $t_n < t < t_{n+1}$;
μ = Dynamic viscosity of the geothermal fluid;
k = Permeability;
h = Reservoir thickness;
t_n = Time at which the flow starts;
t_{n+1} = Time at which the flow stops;
$q(\tau)$ = Volumetric flow rate at time τ;
r = Distance between the observation well and the production well.

6.6 Calibration and simulation of history

The aquifer is assumed to be an infinite, extensive, homogeneous and isotropic system with several production wells at different locations. The skin factor is assumed to be 0. For a production well, the skin

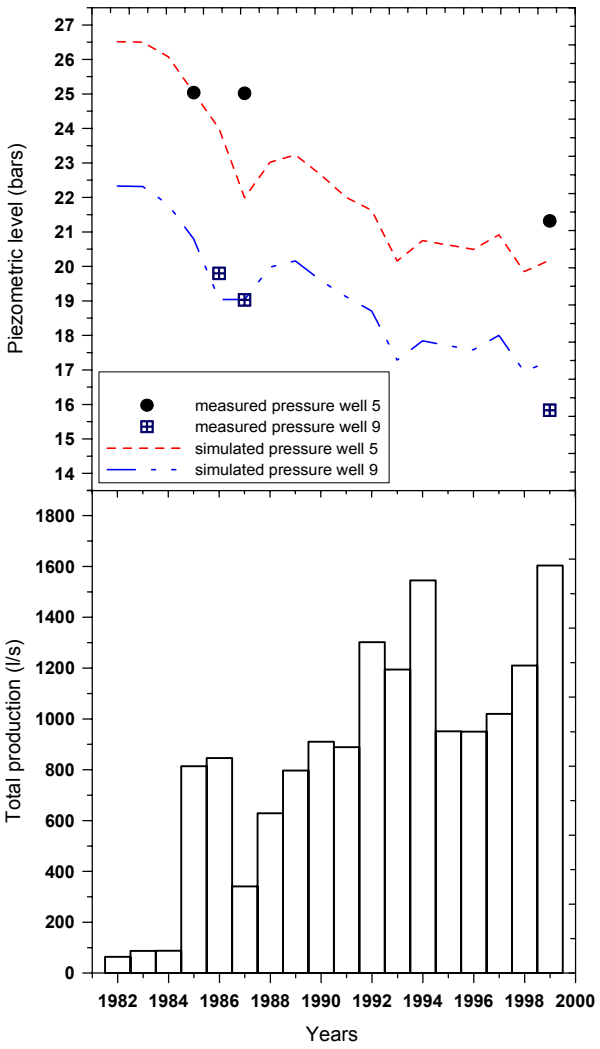

FIGURE 16: Measured and simulated water level changes in wells 5 and 9

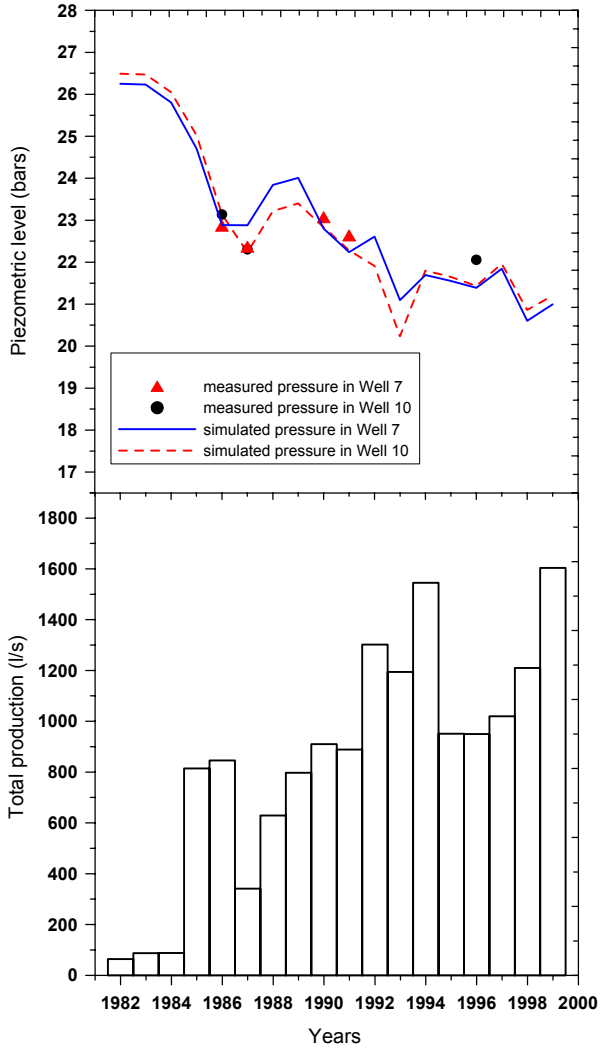

FIGURE 17: Measured and simulated pressure changes in wells 7 and 10

factor average is about zero. The reservoir is assumed to be horizontal. The depth of the wells reaching the main reservoir is from 620 to 2,570 m. The average thickness is assumed to be about 100 m. No boundaries were assumed. The average reservoir temperature is taken to be 70°C. Calibration is obtained by matching simulated to measured pressures as well as possible. The east and north directions were chosen as the X and Y-axes, respectively, with origin placed at well 9. Some production wells were also taken as observation wells.

Examples of calibration simulations are shown in Figures 16 and 17. Additional simulations are shown in Appendix 5. The following parameters were obtained by VARFLOW: X-axis transmissivity = Y-axis transmissivity, or $T_x = T_y = 5\times10^{-6}$ m^3/Pa/s; storativity = 0.4×10^{-9} m/Pa. The piezometric level varies inversely with the total flow rate from the geothermal system. The piezometric level drops when exploitation increases. This relationship is shown in Figure 10. The calculated piezometric level is simulated for some wells, which reach the main feed zone of the C.I. aquifer wells (9, 5, 19, 10, 14). Figures 16 and 17 show the simulated and measured water level in some wells as well as the total production from the reservoir in the Kebili area. The drawdown for all the wells is fairly high during the period from 1982 to 1999. This is caused by the steady increase in total production from the reservoir. The pressure history was simulated for the entire period. Transmissivity T equals kh/μ, and therefore the permeability, k, can be estimated from

$$k = \frac{T\mu}{h} \qquad (11)$$

where k = Permeability [m^2] or [D];
T = Transmissivity 5×10^{-6} [m^3/Pa/s];
h = Thickness of reservoir: 100 [m];
μ = Dynamic viscosity of geothermal water 0.000405 [kg/m/s].

This resulted in a value of $k = 20\times10^{-12}$ m^3 = 20 D. The comparison between well tests and the VARFLOW calculation is shown in Table 5.

TABLE 5: Parameters estimated for analysis

Parameters	Well test	VARFLOW
Transmissivity (10^{-6} m^3/Pa/s)	4.9	5.0
Storage coefficient (10^{-9} m/Pa)	4,1	0.4
Permeability (D)*	20	20

* Using a thickness of 100 m

6.7 Prediction

The simulated drawdown falls rapidly at the beginning and then decreases more slowly (Figures 18 and 19). Two regions with different drawdown can be identified. The first region is located in the northeast (Chott Fejij region) and has an average drawdown of 1 to 1.5 m/year from 1982 to 1991. After 1991 it increases to reach an average of 2 to 3 m/year until 1999. This is due to the rapid growth in the total production from the reservoir caused by the drilling of new wells. In the region, Nefzaoua, the drawdown average is about 1 to 2 m/year, except at well 9 situated close to the Algerian border.

The prediction of piezometric level changes for the next 20 years (Figure 20) is based on the history of production from the reservoir and likely future increases in response to social and demographic changes in the Kebili area as well as in the other Tunisian areas which are able to exploit the C.I. aquifer and in neighbouring Algeria. The scarcity of data from these latter areas limits the accuracy of the prediction results. The prediction of drawdown is based on an immediate increase in production from 1,210 l/s to 1,610 l/s and a constant total flow rate staying constant until year 2020. The prediction is carried out to the year 2020. The predicted drawdown is about 38-40 m in Nefzaoua and 60 m in the Chott Fejij area and at the Algerian border (well 9). The resulting parameters are presented in Table 6.

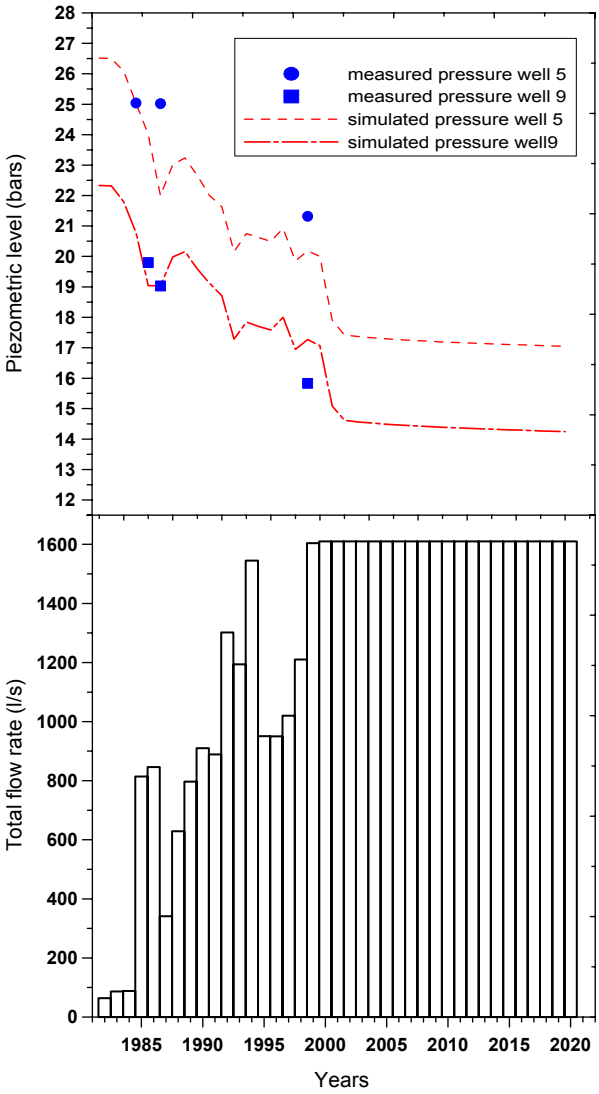

FIGURE 18: Predicted piezometric level for wells 5 and 9

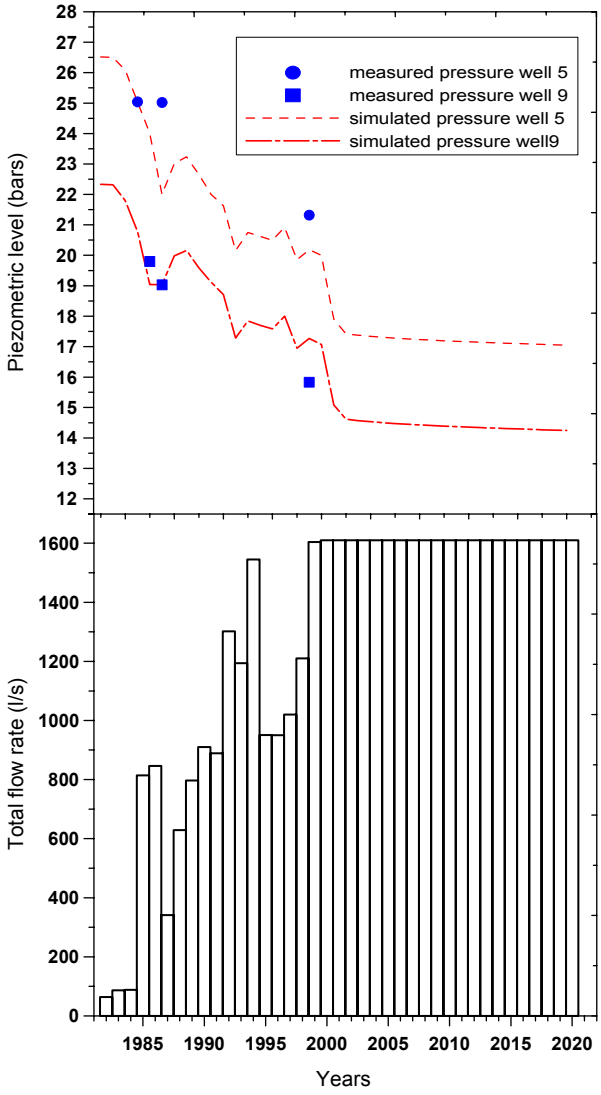

FIGURE 19: Predicted piezometric level for wells 10 and 14

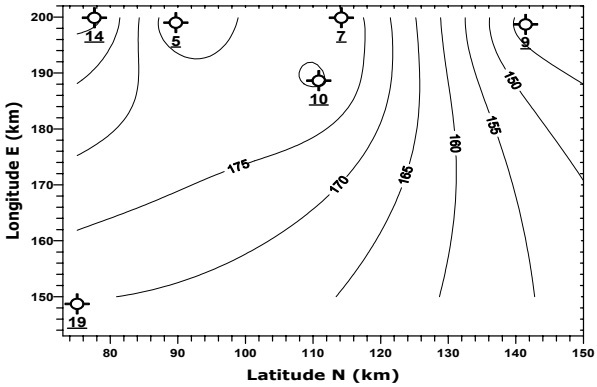

FIGURE 20: Predicted piezometric level contours in year 2020

Figure 20 shows the predicted water level contours in year 2020. This prediction has implications for future needs for pumping because cooling towers are preferentially located on high ground. The maximum drawdown will occur in the Souk Lahad area (in the north of the study area and wells 5, 6, 14, 17 and 22).

TABLE 6: Piezometric level and drawdown predicted by program VARFLOW

Region	Draw-down 1999-2020 (m)	Piezometric level 2020 (bar)
Nefzaoua	38 – 40	18 – 19
Chott Fejij	40 – 60	14.5 – 16.9

7. CONCLUSIONS

The main objectives of this project were to:

1. Determine the principal causes of anchor casing corrosion and to suggest methods of avoiding this problem.
2. To predict to year 2020 the pressure drawdown assuming a moderate increase in production.

The results and recommendations are summarized here below.

7.1 Results

1. Triangular Cl-SO_4-HCO_3 plots of water chemistry data from wells reaching the C.I. show the water to be located midway between the Cl and SO_4 corners. The fluid can, therefore, be classified as sulphate-chloride waters.

2. The isotopic study shows the data points to be concentrated along the meteoric line of Craig (1961) indicating a meteoric origin for the geothermal water. $\delta^{18}O$ ranges from -7.5 to -9% and this signature is characteristic of palaeowaters in northwestern Africa.
3. The main result concerning corrosion is that it is mainly of external origin, i.e. caused by moisture, high temperatures and the presence of salts as well as the pH conditions surrounding the anchor casing and wellhead.
4. Based on a plot of wellhead temperatures, the thermal gradient can be seen to increase from the southeast to the northwest whereas the depth to the top of the producing zone increases from east to west. The total concentration of dissolved salts (TDS) decreases from southeast to northwest.
5. The flow path of geothermal fluid is seen to be from southwest to northeast. The piezometric gradient is about 6 to 10 m/km, respectively, in the north and in the south. Piezometric changes, due to production, are about 1-3 m/year.
6. The simulation by program VARFLOW indicates that transmissivity and storativity of this horizontal and homogeneous reservoir are 5×10^{-6} $m^3/Pa/s$ and 0.4×10^{-9} m/Pa, respectively.
7. Model predictions for year 2020 suggest a water level drawdown of 38-40 m in Nefzaoua and 60 m in the Chott Fejij area and at the Algerian border (well 9). This is based on an optimistic scenario in which production is increased by 400 l/s in year 2000 and kept constant during the following 20 years.

7.2 Recommendations

To avoid external corrosion, several possible methods can be used. A special thickness (17-20 mm) of anchor casing (13 3/8" and 18 5/8") can be used for the topmost pipe. Alternatively, an inhibiting filming agent can be used to cover the anchor casing. The corrosive factors of the environment, such as moisture, temperature, and salts, can be modified chemically or by other means. The material used in wellhead components (API 3000 spec. 6A) should be designed for all expected climatic and environmental conditions (rain, wind, oxygen in the air etc.). Furthermore, the critical part of the anchor casing should be isolated from the corrosive environment i.e. by glanding and/or by filling the surrounding space with some inert material, e.g. cement grout, or coating the surface with a resistant film, e.g. chromium plating.

More detailed study and more research must be carried out on the Continental Intercalaire aquifer. Full collaboration with Algerian and Libyan organisations is necessary in order to achieve economical and sustainable future production and regional development. Long term monitoring of pressures, temperatures and the salinity at the wellhead for each production well should be carried out. Increasing drawdown during the next 20 years caused by increasing production will lead to environmental changes (subsidence, soil salinization, etc.) and should be studied in order to minimize them.

ACKNOWLEDGEMENTS

I would like to express my utmost appreciation to those who played a role and made possible my attendance at the Geothermal Training Programme, especially to Mr. Seddik Saad, regional commissioner of agriculture development of Kebili, Tunisia, to Dr. Ingvar B. Fridleifsson director of the U.N.U. Geothermal Training Programme, for the fellowship award and his excellent guidance and moral support, Mr. Lúdvík S. Georgsson and Mrs. Gudrún Bjarnadóttir for their efficient help and kindness in my daily life and work. Special thanks are due to Mr. Steinar Thór Guðlaugsson, at Orkustofnun, my supervisor, for his generous sharing of time, his experience and critical advice during all stages of my preparation of this modest work and realisation of this report. I'm very grateful to Mr. Sverrir Thórhallsson for his excellent technical support and friendliness. Many thanks are due to the Orkustofnun staff members and lecturers for their kindest help, teaching and assistance during my stay in Iceland.

REFERENCES

Axelsson, G., and Björnsson, G., 1993: Detailed three-dimensional modelling of the Botn hydrothermal system in N-Iceland. *Proceedings of the 18th Workshop on Geothermal Reservoir Engineering, Stanford University, California,* 159-166.

Ben Dhia, H., and Bouri, S., 1995: *Overview of geothermal activities in Tunisia*. Ecole Nationale d'Ingenieurs de Sfax, Tunisia, 5 pp.

Ben Mohamed, M., 1997: Agricultural geothermal utilisation in Kebili region South of Tunisia. Report 2 in: *Geothermal Training in Iceland 1997*. UNU G.T.P., Iceland, 27-56.

Castany, G., 1982: Septentrional Sahara sedimentary basin (Algeria-Tunisia). Continental intercalaire and Complex terminal aquifers (in French). *Bull. BRGM, 2,* 127-147.

Craig, H., 1961: Standards for reporting concentrations of deuterium and oxygen-18 in natural waters. *Science, 133*, 1933-1934.

CRDA, 1999: *Annual reports 1999*. CRDA, Kébili, Tunisia, regional report (in French), 110 pp.

Edmunds, W.M., Shand, P., Guendouz, A.H., Moulla, A.S., Mamou, A. and Zouari, K., 1995: *Recharge characteristics and groundwater quality of the grand erg oriental basin*. British Geological Survey, technical report No. WD/95/44R, Hydrogeology series, 24 pp.

Edmunds, W.M., Shand, P., Guendouz, A.H., Moulla, A.S., Mamou, A. and Zouari, K., 1997: *Recharge characteristics and groundwater quality of the Grand Erg Oriental basin*. British Geological Survey, Wallingford, final report, 9 pp.

Elguedri, M., 1999: Assessment of scaling and corrosion problems in the Kebili geothermal field, Tunisia. Report 1 in: *Geothermal Training in Iceland 1999*, UNU G.T.P., Iceland, 1-40.

ERESS project, 1972: *Water resources study in Septentrional Sahara, vol. 7* (in French). UNESCO, Paris.

Gabolde, G., and Nguyen, J.P., 1999: *Drilling data handbook* (7th edition). Institut Francais de Pétrole Publications, Paris, 552 pp.

Giggenbach, W.F., 1991: Chemical techniques in geothermal exploration. In: D'Amore, F. (coordinatior), *Application of geochemistry in geothermal reservoir development*. UNITAR/UNDP publication, Rome, 119-142.

Hayashi, Y., 1988: *Fundamentals of corrosion*. IGTCGE, Kyushu, Japan, textbook no. 29.

Japan International Cooperation Agency, 1996: *The feasibility study on the irrigated area improvement in oasis in the south of the republic of Tunisia*. Sanyu Consultant Inc. Nippon Koei Co. Ltd., vol. II, draft final report (annexes), 437 pp.

Matthews, C.S., and Russell, D.G., 1967: *Pressure buildup and flow tests in wells*. Soc. Petr. Eng., Monograph vol. 1, 167 pp.

New Zealand Standard, 1991: *Code of practice for deep geothermal wells*. Standards Association of New Zealand, Wellington, NZ, 93 pp.

Speller, F.N., 1935: *Corrosion causes and prevention. An engineering problem*. McGraw-Hill Book Co., Inc., N.Y., 694 pp.

Todd, D.K., 1959: *Ground water hydrology.* John Wiley and Sons, Inc., NY, 336 pp.

Uhlig, H.H., 1967: *Corrosion and corrosion control an introduction to corrosion science and Engineering.* John Wiley & Sons, Inc., NY, 371 pp.

APPENDIX 1: Procedure of coordinates conversion

To transform coordinate data from degrees to km units (UTM units), the following mathematic formulae were used:

$$X_i = \pi R_z \frac{90 - \beta_o}{180} \sqrt{2[1 - \cos\frac{\pi \alpha_{x_i}}{180}]} \quad (1)$$

$$Y_i = \pi R_z \frac{90 - \beta_{y_i}}{180} \quad (2)$$

$$\alpha_i = st\alpha_i + \frac{[\frac{\sec \alpha_i}{60} + \min \alpha_i]}{60} \quad (3)$$

$$\beta_i = st\beta_i + \frac{[\frac{\sec \beta_i}{60} + \min \beta_i]}{60} \quad (4)$$

where α_i = Conversion of longitude from UTM unit;
β_I = Conversion of latitude from UTM unit;
R = Radius of the earth: 6 371,299 m;
α_o = Minimum value of longitude: 8°;
β_o = Minimum value of latitude: 32°.

Wells	Longitude (°)	Latitude (°)	Longitude (km)	Latitude (km)
C.I.11	9°00’ 47”	33°33’ 11.3”	114,026	172,709
C.I.16	9°00’ 30”	33°40’54”	113,510	187,002
C.I.10	8°59’5.3”	33°41’56.5”	110,855	188,623
C.I.3	8°56’47”	33°43’25.4”	106,543	191,678
C.I.13	8°56’37”	33°43’6.8”	106,209	191,104
C.I.12	9°01’59”	33°26’9.7”	116280	159,686
C.I.18	9°00’52”	33°24’27.6”	114,195	156,533
C.I.1	8°50’6,6”	33°46’39.6”	94,011	197,677
C.I.2	8°46’4.6”	33°47’28.8”	86,444	199,197
C.I.14	8°44’33”	33°47’50.8”	77,658	199,876
C.I.4	8°49’50”	33°47’9.1”	93,489	198,588
C.I.19	8°40’1.8”	33°20’14.5”	75,100	148,715
C.I.17	8°43’22”	33°48’41.1”	81354	201430
C.I.8	9°04’46”	33°46’6.4”	121,517	196,651
C.I.7	9°00’52”	33°47’51.1”	114,185	199,885
C.I.9	9°15’24”	33°47’12.4”	141,444	198,690

APPENDIX 2: Production and pressure history of wells reaching C.I. aquifer in Kebili area, Tunisia

TABLE 1: Location of Kebili wells and wells' characteristics

Well no.	Location												Wells characteristics				
	Latitude(N)			Longitude(E)			French system						Alt.	Depth	S.L.	Q	Drill. year
							Latitude(N)			Longitude(E)							
	deg.	min.	sec.	deg.	min.	sec.	gr.	min.	sec.	gr.	min.	sec.	(m)	(m)	(m)	(l/s)	
1	33	46	39.6	8	50	6.6							42.39	1,420	20.9	18	1983
2	33	47	28.8	8	46	4.6							26.52	1,405	38.6	28	1984
3	33	43	25.4	8	56	47							31.54	2,200	56.5	14	1985
4	33	47	9.1	8	49	50							39.05	2,200	205.9	79	1985
5	33	47	19.4	8	47	49.6							38.17	2,229	212.2	84	1985
6	33	46	53.9	8	51	35.8							38.75	2,310	202.3	86	1986
7	33	47	51.1	9	00	52							50.37	1,987	178.5	50	1986
8	33	46	6.4	9	04	46							81.98	1,752	152.9	46	1985
9	33	47	12.4	9	15	24							53.31	1,621	137.3	58	1986
10	33	41	56.5	8	59	5.3							55.57	2,580	176	77	1986
11	33	33	11.3	9	00	47							44.22	2,162	217.2	126	1986
12	33	26	9.7	9	01	59							63.68	2,080	198.2	36	1986
13	33	43	6.8	8	56	37							-	2,682	197.3	30	1992
14	33	47	50.8	8	44	33							-	2,480	217.5	32	1992
16	33	40	54	9	00	30							-	2,800	139.3	110	1994
17	33	48	41.1	8	43	22							-	2,500	205	108	1994
18	33	24	27.6	9	00	52							-	2,020	186	114	1994
19	33	20	14.5	8	40	1.8							-	1,894	211.7	30	1993
20							37	54	70	7	19	80	-	1,104	12.1	55	1999
21							37	54	00	7	24	30	-	1,099	5,3	83	2000
22							37	54	70	7	17	45	-	2,358	188.5	219	2000
23							37	49	10	7	69	12	-	1,245	21.2	55	1999
AG1							37	55	71	7	39	88	-	82	2.15	10	1993
AG3							37	55	50	7	36	60	-	60	7.65	33	1993
KG2	33	59	13.0	9	38	21							-	676	-	57	1963
KG3	33	59	12.5	9	38	21							-	680	69.4	69	1980
Mbs							36	48	00	8	11	00	236.1	680	57.5	5	1986
Mch							37	54	25	7	21	15	33.21	1,495	62	16	1949
OF2	33	47	56.4	9	13	17							48.28	904	-	36	1952
OF3	33	47	3.5	9	14	4.8							39.18	503	31.4	14	1955
Sa	33	45	9.7	9	17	42							85.53	745	73.6	28	1985
St2	33	48	0.7	9	00	43							48.76	52	-	7	1961
St3	33	48	0.7	9	00	43							47.14	1,005	56.6	13	1961

TABLE 2: Production and pressure decline history for the Kebili wells

Well	1982		1983		1984		1985		1986		1987		1988		1989		1990	
no.	Q(l/s)	P(m)	Q(l/s)	P(m)	Q(l/s)	P(m)	Q(l/s)	P(m)	Q(l/s)	P(m)	Q(l/s)	P(m)	Q(l/s)	P(m)	Q(l/s)	P(m)	Q(l/s)	P(m)
1			18	+20.9			32				-		30		28		24	
2					28	+38.6	35	+56.5	51		-		46		43		34	
3							35	+43	34		35	+55.5	35	+50	30		23	
4							30	+205.9	75		50	+205.9	35		80		85	
5							84	+212.2	60		26	+212	25		80		92	
6							85		86	+202	-	+202	25	+210	72		80	+195
7							50	+176	50	+178.5	15	+178	20		35		40	+178.7
8							40	+152.9	25	152	30	+151.2	30		40		40	
9							60		58	+137.3	30	+137	25		35		50	
10							85		80	+175.80	80	+167.5	85		35		81	
11							-		126	+217.2	15		31		80		80	
12							45	+176	20	+198.2	-		30		36		46	+198
13							-		-		-		-		-		-	
14							-		-		-		-		-		-	
16							-		-		-		-		-		-	
17							-		-		-		-		-		-	
18							-		-		-		-		-		-	
19							-		-		-		-		-		-	
20							-		-		-		-		-		-	
21							-		-		-		-		-		-	
22							-		-		-		-		-		-	
23							-		-		-		-		-		-	
AG1							-		-		-		-		-		-	
AG3							-		-		-		-		-		-	
KG2							65				-		70		68		69	
KG3	64	+70.8	69	+68	60	+67.9	80	+65	70		60	-	58	-	68	-	66	+66
Mbs							5	+57.5	5	+57.5	-		5		9		9	
Mch							4				-		-		-		4	
OF2							10		7		-		9		7		8	
OF3							30		60		-		33		8		30	
Sa							28	74	25		-		16		26		28	
St2							0		14		-		8		7		8	
St3							12		13		-		12		11		12	

TABLE 2: Continued

Well	1991		1992		1993		1994		1995		1996		1997		1998		1999	
no.	Q(l/s)	P(m)	Q(l/s)	P(m)	Q(l/s)	P(m)	Q(l/s)	P(m)	Q(l/s)	P(m)	Q(l/s)	P(m)	Q(l/s)	P(m)	Q(l/s)	P(m)	Q(l/s)	P(m)
1	17		17		18		18		16		37		37		37		37	
2	27		27		31		28		18		25		20		35		28	
3	35	+43	32		18		9		6		-		-		22		21	
4	60		83		69		55		63		60		61		67		42	
5	90		85		86		84		71		66		63		57		69	+175
6	80		81		90		86		57		54		55		50		47	
7	50	+176	50		54		50		54		50		49		47		54	
8	50		50		52		46		57		39		40		46		41	
9	20		48		53		58		49		29		31		38		45	+105
10	85		85		72		71		74		76	+165	65		57		56	
11	97		80		105		126		116		112		122		110		98	
12	45		45		36		36		11		23		52		72		56	
13	-		180	+197.3	30		30		30		36		66		57		45	+175
14	-		211	+217.5	32		32		36		35		51		84		86	+190
16	-		-		-		110	+139.3	-		-		-		-		40	
17	-		-		-		215	+205	-		-		-		-		30	
18	-		-		-		228	+186	-		-		-		58		75	
19	-		-		230	+211.7	30		50		53		45		101		60	+180
20	-		-		-		-		-		-		-		-		-	+12.1
21	-		-		-		-		-		-		-		-		-	-
22	-		-		-		-		-		-		-		-		-	-
23	-		-		-		-		-		-		-		-		-	+21.2
AG1	-		-		3		2		2		2		2		2		2	
AG3	-		-		-		2		2		1		27		20		21	
KG2	65		67		63		52		65		64		44		61		57	
KG3	80	+65	75		68		69		74		64		80		85		48	
Mbs	6		4		7		5		5		15		10		8		5	+48
Mch	4		4		4		14		14		20		20		21		18	
OF2	8		9		5		5		6		6		6		4		6	
OF3	30		30		18		36		35		38		36		35		31	
Sa	26		26		28		28		22		20		20		20	+190.5	20	
St2	0		0		7		7		8		14		9		9		10	
St3	12		13		15		13		13		12		12		10		9	

APPENDIX 3: Analytical results of minor elements (µg/litre) (Edmunds et al., 1995)

Well	pH	Mn	F	Br	I	Ptotal	Li	Be	B	Al	Sc	V	Cr	Co	Ni	Cu
C.I:4	7.9	0.030	0.6	0.736	0.0503	<0.5	160	<1.4	320	2.9	<2	<20	<0.98	<0.82	4.9	7.9
C.I:5	8.0	0.036	0.7	0.760	0.0500	<0.5	168	<1.4	340	1.8	3	20	<0.98	<0.82	6.0	10.5
C.I:6	8.1	0.444	0.5	0.783	0.1170	<0.5	144	<1.4	450	2.3	<2	<20	<0.98	<0.82	5.5	3.6
C.I:7	8.1	0.065	0.6	0.776	0.049	<0.5	149	<1.4	290	<2.1	<2	<20	<0.98	<0.82	21.4	3.1
C.I:8	8.3	0.014	0.6	0.912	0.0530	<0.5	152	<1.4	370	54.6	<2	<20	<0.98	<0.82	6.5	3.2
C.I:9	8.3	0.020	0.6	0.846	0.0499	<0.5	165	<1.4	360	3.3	<2	<20	<0.98	<0.82	5.9	5.4
C.I:10	8.2	0.027	0.5	1.100	0.0629	<0.5	166	<1.4	500	<2.1	<2	<20	<0.98	<0.82	5.8	7.4
C.I:11	8.2	0.034	0.6	1.590	0.0596	<0.5	214	<1.4	660	<2.1	<2	<20	<0.98	<0.82	6.1	3.0
C.I:12	8.2	0.072	0.6	2.620	0.0682	<0.5	279	<1.4	1000	6.3	14	90	<0.98	<0.82	7.4	7.1
C.I:14	8.0	0.023	0.7	0.720	0.0517	<0.5	151	<1.4	330	<2.1	<2	<20	<0.98	<0.82	5.2	3.3
Mbs	8	0.010	0.7	3.040	0.0695	<0.5	160	<1.4	610	2.1	<2	<20	<0.98	<0.82	7.4	5.3
KG3	7.7	0.028	2.2	0.744	0.0847	<0.5	120	<1.4	620	63.1	<2	<20	<0.92	<0.82	13.2	5.0

Well	Zn	Gn	Go	Rb	Sr	Y	Zr	Mo	Cd	Sb	Cs	Ba	La	Ti	Pb	Bi	U
C.I:4	<3.4	<1.7	<1.5	17	4620	<0.9	<27	4.2	<0.9	<3	<1.4	63.2	<1.25	<1.7	<0.92	<2.7	<0.7
C.I:5	<3.4	<1.7	<1.5	16.7	4560	<0.9	<27	4.6	<0.9	<3	<1.4	69.2	<1.25	<1.7	<0.92	<2.7	<0.7
C.I:6	<3.4	<1.7	<1.5	32.2	6670	<0.9	<27	<3.9	<0.9	<3	<1.4	37.8	<1.25	<1.7	<0.92	<2.7	<0.7
C.I:7	4.7	<1.7	<1.5	16.7	4460	<0.9	<27	<3.9	<0.9	<3	<1.4	61.9	<1.25	<1.7	<0.92	<2.7	<0.7
C.I:8	7.1	<1.7	<1.5	15.4	4660	<0.9	<27	<3.9	<0.9	<3	<1.4	62	<1.25	<1.7	<0.92	<2.7	<0.7
C.I:9	<3.4	<1.7	<1.5	16.2	4680	<0.9	<27	4.4	<0.9	<3	<1.4	54.1	<1.25	<1.7	<0.92	<2.7	<0.7
C.I:10	8.7	<1.7	<1.5	14.2	4410	<0.9	<27	4.3	<0.9	<3	<1.4	50.5	<1.25	<1.7	<0.92	<2.7	<0.7
C.I:11		<1.7	<1.5	15.5	4200	<0.9	<27	5.5	<0.9	<3	<1.4	36.3	<1.25	<1.7	<0.92	<2.7	<0.7
C.I:12	<3.4	<1.7	<1.5	16.6	4590	<0.9	<27	9.7	<0.9	<3	<1.4	36.3	<1.25	<1.7	<0.92	<2.7	<0.7
C.I:14	<3.4	<1.7	<1.5	17.6	4370	<0.9	<27	4.9	<0.9	<3	<1.4	70.6	<1.25	<1.7	<0.92	<2.7	0.7
Mhbs	<3.4	<1.7	<1.5	22.5	6740	<0.9	<27	<3.9	<0.9	<3	<1.4	24.4	<1.25	<1.7	<0.92	<2.7	1.0
KG3	3.8	<1.7	<1.5	19.9	8870	<0.9	<27	9.5	<0.9	<3	<1.4	21.3	<1.25	<1.7	1.10	<2.7	1.0

APPENDIX 4: Solubility of oxygen in distilled water in contact with air

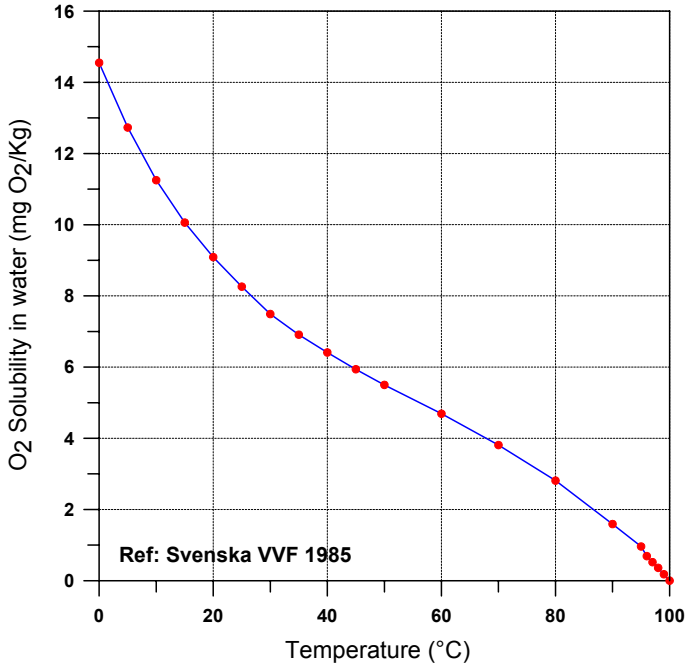

APPENDIX 5: Measured and simulated piezometric level for some wells reaching C.I. aquifer in Kebili area, Tunisia

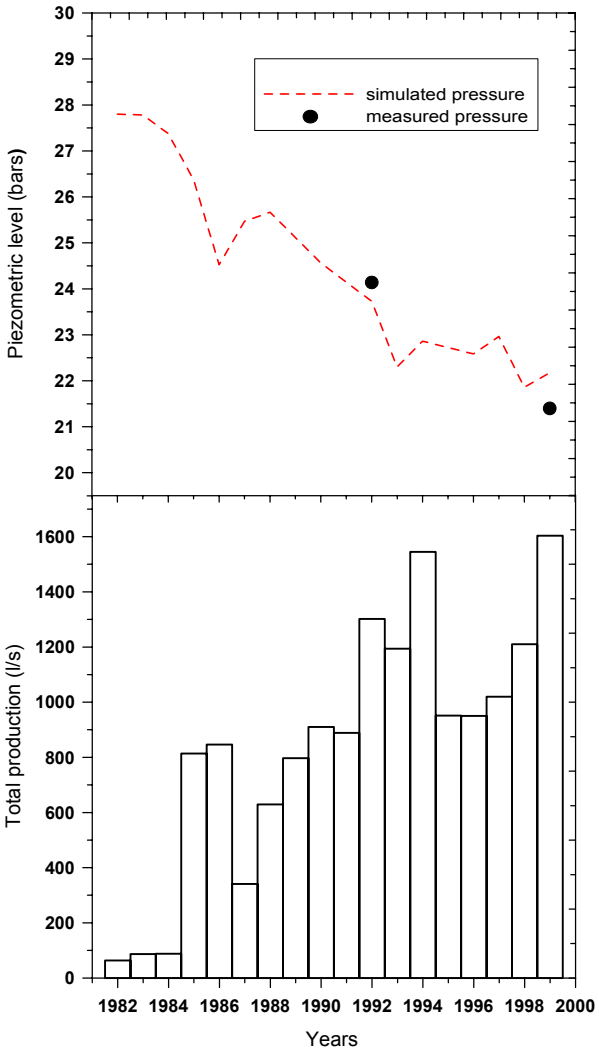

FIGURE 1: Simulated piezometric levels in well 14

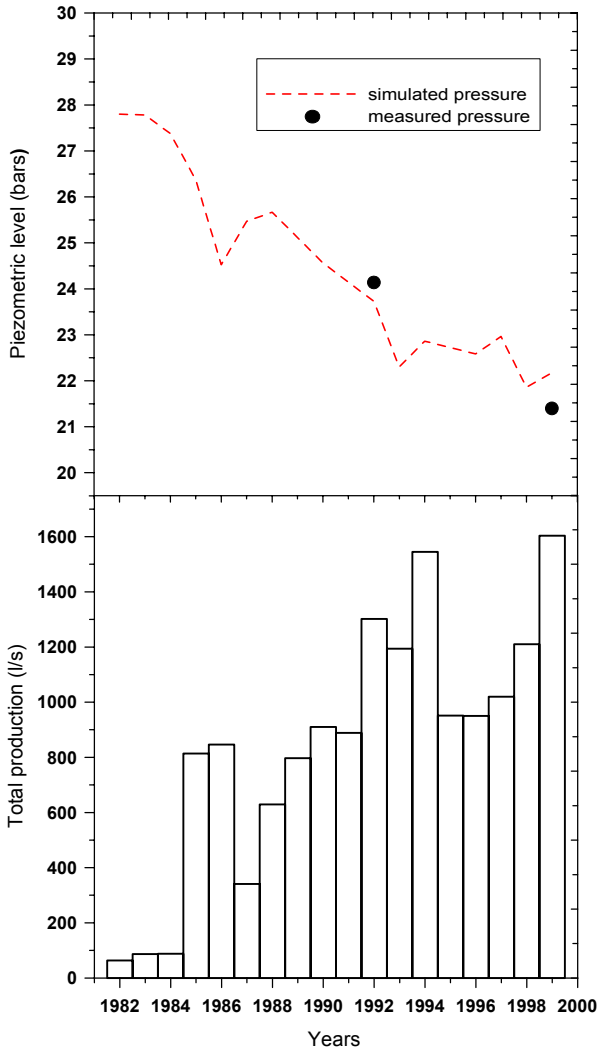

FIGURE 2: Simulated piezometric levels in well 19

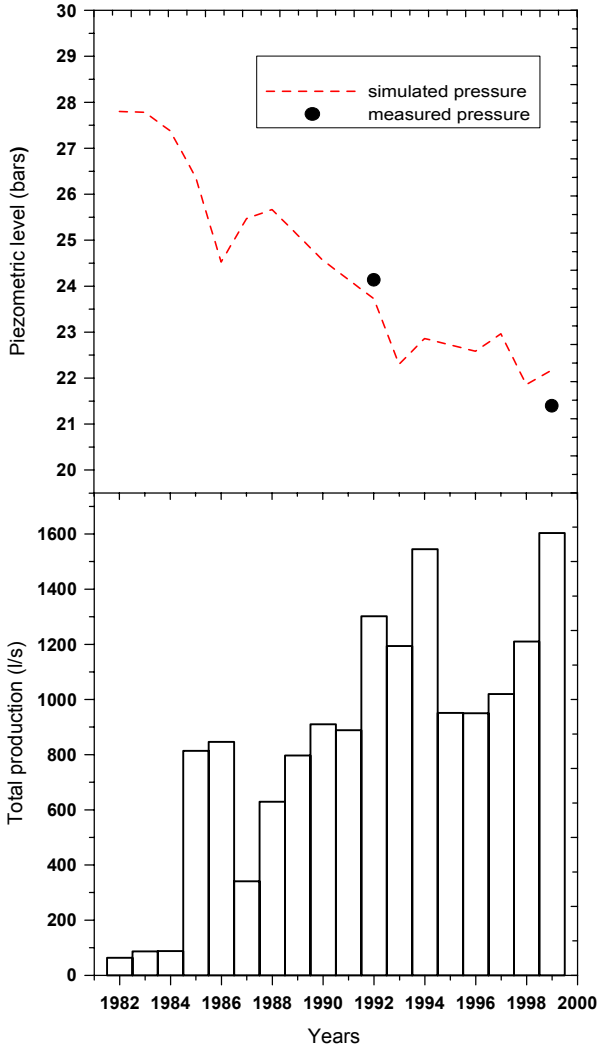

FIGURE 3: Predicted piezometric level in well 7

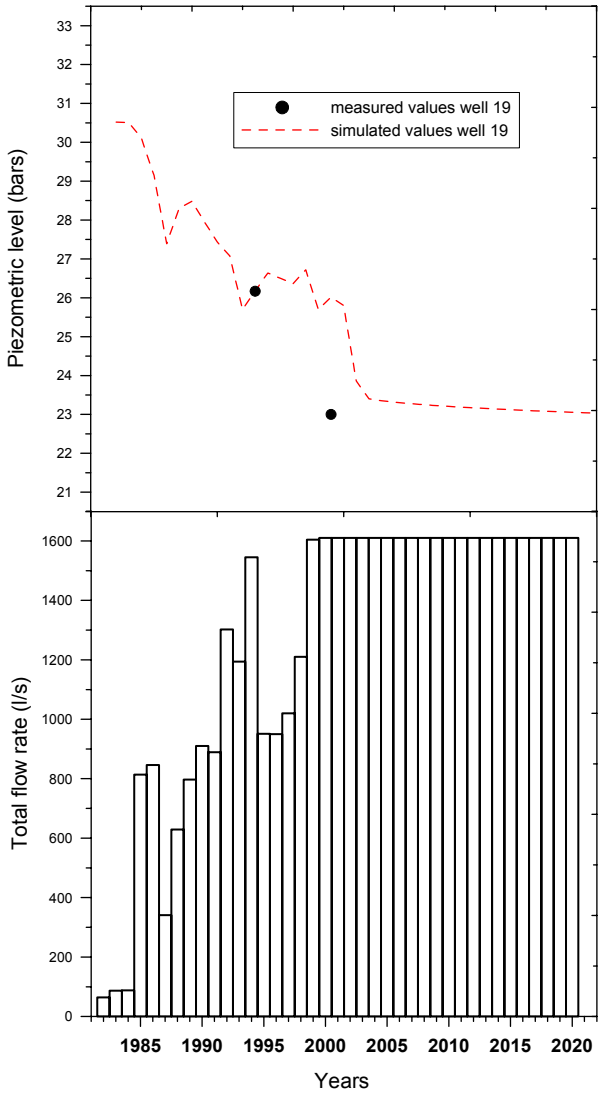

FIGURE 4: Predicted piezometric level in well 19